A New Aerodynamic Data Dispersion Method for Launch Vehicle Design (Invited)

Jeremy T. Pinier*

NASA Langley Research Center, Hampton, VA, 23681–2199

A novel method for implementing aerodynamic data dispersion analysis is proposed. A general mathematical approach, combined with physical modeling tailored to the aerodynamic quantity of interest, enables the generation of more realistically relevant dispersed data and, in turn, more reasonable flight simulation results. The method simultaneously allows for the aerodynamic quantities and their derivatives to be dispersed given a set of non-arbitrary constraints, which stresses the controls model in more ways than with the traditional bias up or down of the nominal data within the uncertainty bounds. The adoption and implementation of this new method within the NASA Ares I Crew Launch Vehicle Project has resulted in significant increases in predicted roll control authority and lowered the induced risks for flight test operations. One direct impact on launch vehicles is a reduced size for auxiliary control systems and the possibility of an increased payload. This technique has the potential of being applied to problems in multiple areas where nominal data together with uncertainties are used to produce simulations using Monte Carlo type random sampling methods. It is recommended that a tailored, physics-based dispersion model be delivered with any aerodynamic product that includes nominal data and uncertainties in order to make flight simulations more realistic and allow for leaner spacecraft designs.

Notice to the Reader

The Ares I launch vehicle, including its predicted performance and certain other features and characteristics, have been defined by the U.S. Government to be Sensitive But Unclassified (SBU). To comply with SBU restrictions, details have been removed from some plots and figures. Despite these alterations, there is no loss of meaningful technical content.

Nomenclature

Symbols

C_i	aerodynamic coefficient
C_l	aerodynamic rolling moment coefficient
$\widetilde{C_l}$	dispersed aerodynamic rolling moment coefficient
ϵ_i	randomly generated dispersion factor
g_i	randomly generated dispersion function
L_b	bias limit
U	uncertainty magnitude
$UCLL$	uncertainty in rolling moment coefficient
ϕ_a	aerodynamic roll angle, degrees

---

*Research Aerospace Engineer, Configuration Aerodynamics Branch, MS 499, Senior Member AIAA.

American Institute of Aeronautics and Astronautics

Acronyms

CFD   computational fluid dynamics
DAC   design and analysis cycle
GNC   guidance, navigation and control
LAS   launch abort system
OML   outer mold line
RCS   reaction control system
RoCS   roll control system
UHF   ultra high frequency

Introduction

During each iterative design cycle of a launch vehicle, aerodynamic databases are provided to the guidance, navigation and control (GNC), and flight mechanics (FM) teams as an input to the flight simulations that predict the vehicle trajectory and performance throughout all phases of flight. The inputs to GNC models come from multiple disciplines on launch vehicles and most inputs are provided as nominal values with uncertainty intervals about the nominal values. In order to design robust control laws and ensure a successful flight test of the vehicle, thousands of Monte Carlo simulations are performed by independently dispersing all model inputs within their uncertainty bounds and ideally predicting all possible events during flight. The resulting predicted performance is analyzed and compared to predefined metrics that determine success or failure for each computed flight simulation. As long as a certain level of success for each given metric is not met, some level of redesign is needed, and the vehicle must undergo as many iterative design cycles as needed until all metric requirements are met with a prescribed level of success. In the best cases, control laws can be redesigned to reduce the number of failures to fewer than the predefined success threshold. In the worst cases, the simulation results might require spending a significant amount of time and resources into understanding the uncovered problems in order to reduce the initial uncertainties and perhaps improve the simulation results. When a better understanding of the problem and reduced uncertainties do not improve flight simulation results, then outer mold line (OML) or hardware redesign could be required, the least desirable situation. Hanson & Beard[1] describe in detail the GNC methodology for applying Monte Carlo simulations in the context of launch vehicle design.

Traditionally, aerodynamic databases consist of: 1) a set of nominal coefficients that are a function of a number of variables and 2) an uncertainty model that is usually a function of a subset of these variables. This paper shows that a physically meaningful dispersion model is highly beneficial to enable realistic modeling of the aerodynamic data within the flight simulations. The adverse effects of an inappropriate dispersion model can have much more of an impact on vehicle performance than the actual uncertainty magnitudes. In cases where uncertainties about the nominal values are large, the absence of a physics-based dispersion model could lead to non-realistically dispersed data and artificially distorted simulation results that will not accurately represent the launch vehicle's behavior in flight.

Much attention has traditionally been placed on the actual magnitude of the uncertainty bounds with respect to the nominal data as a culprit for the vehicle performing poorly in flight simulations when, oftentimes, it is the way by which the nominal data is dispersed that greatly affects the performance results. Simplistic dispersion models may not only introduce unrealistic vehicle behaviors, but they may also omit to stress the model in ways that it should be stressed to better simulate the natural behavior of a vehicle during a real flight. Within large programs, it has however been a challenge to provide more sophisticated dispersion models along with the nominal data and its uncertainty in a way that GNC groups can readily implement and be confident that their results are indeed more representative of reality. In the natural flow of data among disciplines within a development project, the aerodynamics team ought to be required to provide not only nominal data with uncertainties but also dispersion models that, to the best of the aerodynamicists' knowledge, faithfully represent the physical response of the vehicle to its aerodynamic environment. This is one of the Constellation Program lessons learned related to the quantification and use of uncertainty analysis for aerodynamics. More details on the most important lessons learned during this program are reported by Walker et al.[2]

This paper presents in a first part the proposed general mathematical method that enables the creation

American Institute of Aeronautics and Astronautics

of pseudo-random dispersion functions that, by construction, satisfy physical constraints imposed by the vehicle geometry, the features of the nominal data, and the general knowledge gained from the statistical analysis and uncertainty quantification process. The second part provides practical examples of applications of this method to development launch vehicles at NASA and provides insight into additional potential areas where controlled variations and constrained randomness could enhance analysis methods for an improved overall vehicle analysis and design.

I. Dispersion Methodology

Any set of data that has been generated to simulate reality should be attributed a level of uncertainty. If x is a system variable, $f(x)$ is a model that, to the best of the engineer's knowledge, represents the response of the function f to the variable x. Whether the measurements come from an experiment, a computer simulation, or an analytical method, reality always contains a level of variability with respect to the measurements that were performed in a more or less controlled environment, at smaller scales, and/or using approximated engineering methods or simplified models. As shown in Fig. 1, two ways to present this type of "uncertain" data are to provide either a nominal function with uncertainty bounds about the nominal data (left), or simply a band of data (right). In many cases, for design purposes, it is convenient to provide a nominal function, as shown on the left in Fig. 1.

This paper describes various ways of "sampling" this type of data to generate multiple functions, $f_i(x)$, that lie within the uncertainty and that, with enough samples i, will cover the entire band of uncertainty to explore most of the possible outcomes.
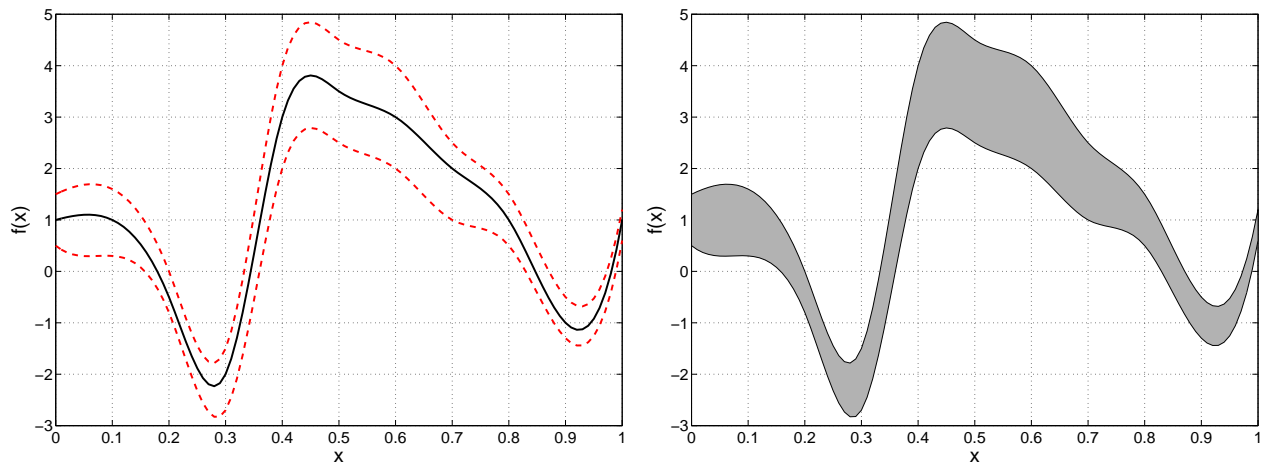

Figure 1. Two ways to provide a dataset with uncertainty: (left) a nominal function and two asymmetric uncertainty bounds, or (right) a band of data bounded by an upper and a lower function.

A. Traditional Method

The traditional dispersion method consists in a shift (or offset) of the nominal data by a randomly generated fraction of the uncertainty. This simple model enables very good control of the distribution of the dispersed data within the uncertainty bounds by prescribing a sampling distribution to the randomly generated factor. The probability distribution of the factor can be prescribed to be either gaussian or uniform, depending on the nature of the data. The following equation illustrates the traditional dispersion method on a generic nominal function, $f(x)$:

$$\widetilde{f}(x) = f(x) + \epsilon_i \ U(x) \tag{1}$$

American Institute of Aeronautics and Astronautics

where $\widetilde{f}(x)$ is the dispersed function, $U(x)$ is the uncertainty that, in general, can be a function of x. The ϵ_i is a randomly sampled uncertainty factor with $-1 \leq \epsilon_i \leq 1$. When thousands of ϵ_i are sampled from a particular probability distribution, this method will, in effect, cover the uncertainty band with the same distribution. Figure 2 illustrates how a function is dispersed using the traditional method. On the left are
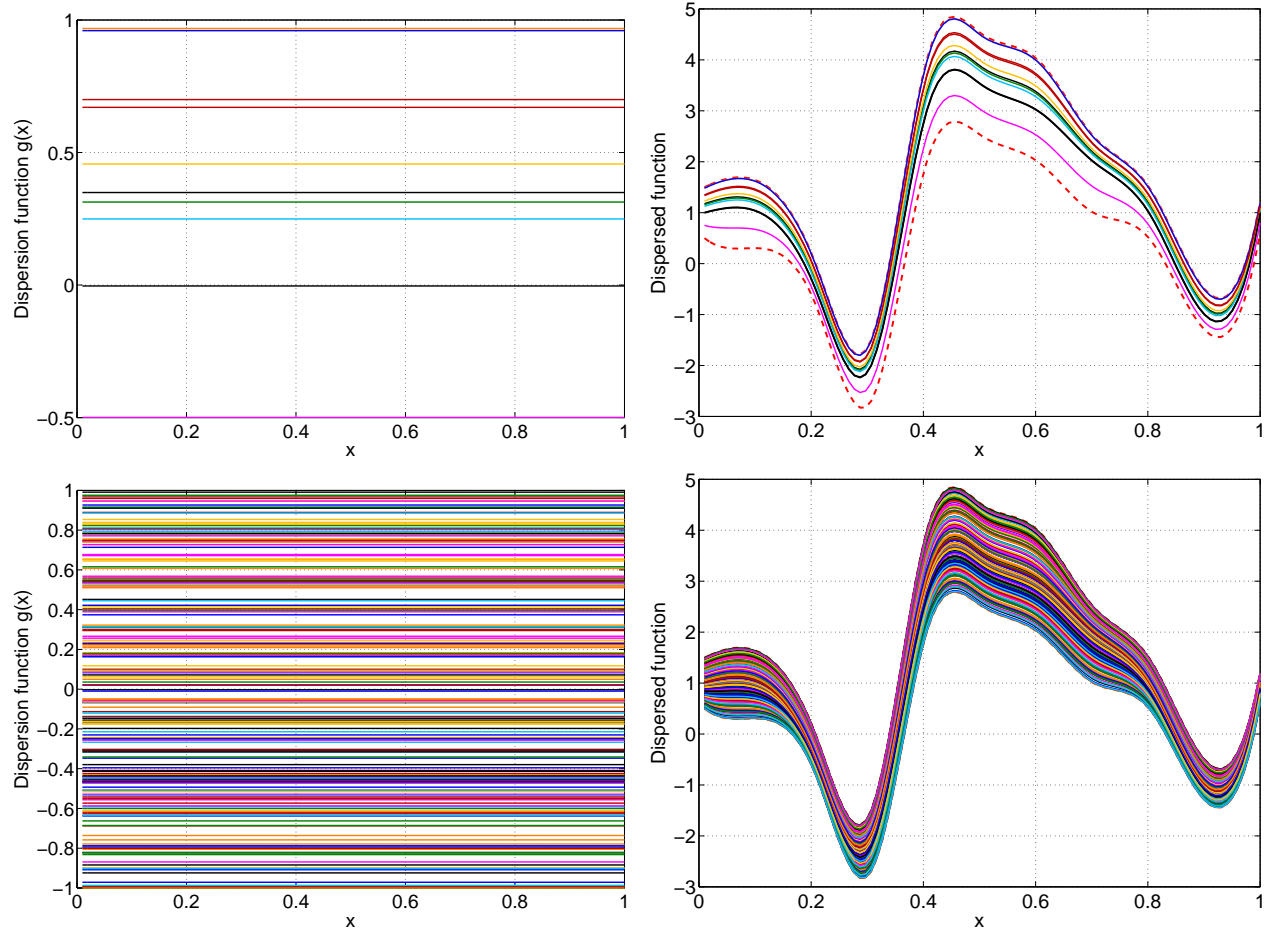

Figure 2. Ten (top) and one hundred (bottom) randomly generated dispersion functions (left) and dispersed functions (right), red dashed lines are asymmetric uncertainty bounds.

shown the dispersion functions $g(x) = \epsilon_i$, and on the right are shown the dispersed functions $\widetilde{f}(x)$ contained within the prescribed uncertainty bounds $U(x)$. Even though this method enables a simple way of filling the uncertainty space with a prescribed distribution, one of the predominant features of this method is the stiff way by which the functions are dispersed. Some of the pitfalls of this method are:

1. It does not allow for phase shifts of the nominal function, i.e., the local peaks of all dispersed functions will be at the same abscissa as the local peaks of the nominal function. Knowledge of the exact location of peaks in a given sample of data should contain uncertainty, and this feature should be modeled.

2. The gradient variation of the dispersed functions is limited by the local difference between the gradients of the uncertainty bounds. In the common cases where the uncertainty bounds are parallel (i.e., symmetric uncertainty distribution), the dispersed functions will not exhibit any gradient variation as compared to the nominal function. Measurement of the slope is also one that contains uncertainty, and that should be modeled as well.

3. In particular applications, as shown in Section II, a simple data offset can lead to unrealistic results because of the fact that the uncertainty bounds themselves are not necessarily realizable observations. They are only the result of single-point statistical uncertainty quantification and do not take into account physical constraints that could limit the sampling possibilities within these bounds. More

American Institute of Aeronautics and Astronautics

details and a practical example are provided in Section II. This is the main reason why the traditional dispersion method will in many cases lead to hyper-conservative flight simulation results.

This traditional dispersion method is widely used in the aerospace community, when Monte Carlo simulations are applied to data with uncertainty to explore all possible outcomes given a set of data. The following section proposes a new dispersion model that not only allows the data to fill the entire uncertainty space but also enables slope variation, as well as phase shifts, and also enables constraints to be set to limit the amount of bias introduced by the dispersed functions. This allows for a safer and leaner design, because the vehicle is modeled in a more realistic way, and non-physical biases can some times lead to over-sizing actuators and structures.

B.   New Dispersion Method

Prediction data can be removed from the truth in two ways: (1) bias error and (2) random error. It can also be a combination of the two. The traditional model only allows for bias errors to be modeled in the dispersed functions. The model proposed in this paper allows for both bias and random error to be modeled at the same time while remaining constrained by the provided uncertainty bounds. In addition to the constant offset dispersion term ϵ_i as shown in Eq. 1, the new dispersion model introduces an additional uncertainty term with a functional dispersion factor $g_i(x)$, as follows:

$$\widetilde{f}(x) = f(x) + \epsilon_i \ L_b \ U(x) + (1 - |\epsilon_i \ L_b|) \ g_i(x) \ U(x) \tag{2}$$

where $\widetilde{f}(x)$ is the dispersed function. $U(x)$ is the uncertainty magnitude, ϵ_i is a randomly sampled uncertainty factor with $-1 \le \epsilon_i \le 1$. L_b is the bias limit, with $-1 \le L_b \le 1$ and the dispersion function $g_i(x)$ is a randomly generated dispersion function that satisfies $-1 \le g_i(x) \le 1$. The new dispersion model allows for the presence of a bias uncertainty limited to a magnitude of $L_b * U(x)$, with the remaining uncertainty band allowed to be modeled as a pseudo-random function of x. The following partial sum of Fourier series is the proposed general model for the dispersion function $g_i(\bar{x})$:

$$g_i(\bar{x}) = \sum_{k=1}^{N} (a_k \ sin \left(2\pi \ (k \ \bar{x} + h_k)\right) + b_k \ cos \left(2\pi \ (k \ \bar{x} + h_k)\right)) \tag{3}$$

where a_k, b_k and h_k are randomly generated real numbers uniformly distributed between -1 and 1, and $\bar{x}$ varies on a normalized scale from 0 to 1. N is the order of the partial Fourier series. The a_k and b_k coefficients are the random magnitudes of the sines and cosines, respectively, and the h_k coefficients are the random phases. The random phase enables the uncertainty band to be fully covered by the dispersed functions. Two parameters need to be chosen a priori to implement this model: the order of the Fourier series, N, and the bias limit, L_b. It is shown here how these parameters can be determined, based on a combination of physical reasoning and empirical data analysis:

1. **The order of the partial Fourier series,** N: It is argued that any randomly dispersed function should exhibit a frequency content of the same order as that of the nominal function itself. Therefore the order of the series should not be higher than half the number of local extrema in the nominal function. As an example, the nominal function in Fig. 2 contains on the order of 4 local extrema and, therefore, the model should be of order $N = 2$.

2. **The bias limit,** L_b: In most cases, it is unrealistic to assume that 100% of the uncertainty could be due to systematic error and, therefore, be modeled by a simple bias. In some cases, a strong physical argument can be made to justify setting the bias limit to zero (as is the case in the Ares I rolling moment example provided in the following section). However, most of the time, a portion of the uncertainty can be attributed to systematic errors, and the remaining portion attributed to randomized error sources. An empirical study of the available data (from flight tests, wind tunnel tests, and computational fluid dynamics) and an engineering argumentation to determine the potential sources of systematic and randomized errors are required to determine the magnitude of the bias limit L_b.

In addition, the dispersion function is constrained by: $|g_i(x)| \le 1$, so that every dispersed function remains within the predefined uncertainty bounds. As shown in Eq. 3, this model does not satisfy this constraint. There are two ways to force all dispersed functions $g_i(x)$ to be smaller than 1 in absolute value.

- **The 'redraw' method:** In the redraw method, any generated dispersion function that does not satisfy $|g_i(x)| \leq 1$ for all x is discarded, and a new function is generated until the required number of dispersion functions are generated.

- **The 'scaling' method:** In the scaling method, any generated dispersion function that does not satisfy $|g_i(x)| \leq 1$ for all x is normalized by its maximum value to force the constraint to be satisfied for every generated dispersion function. This method is slightly faster since all the functions that are generated will satisfy the constraint, by means of a normalizing factor; however, both methods are computationally fast on a desktop computer (on the order of seconds for 2000 random functions). When using the scaling method, the distribution of the dispersed functions will be heavily weighted at the uncertainty limits because of the normalizing process.
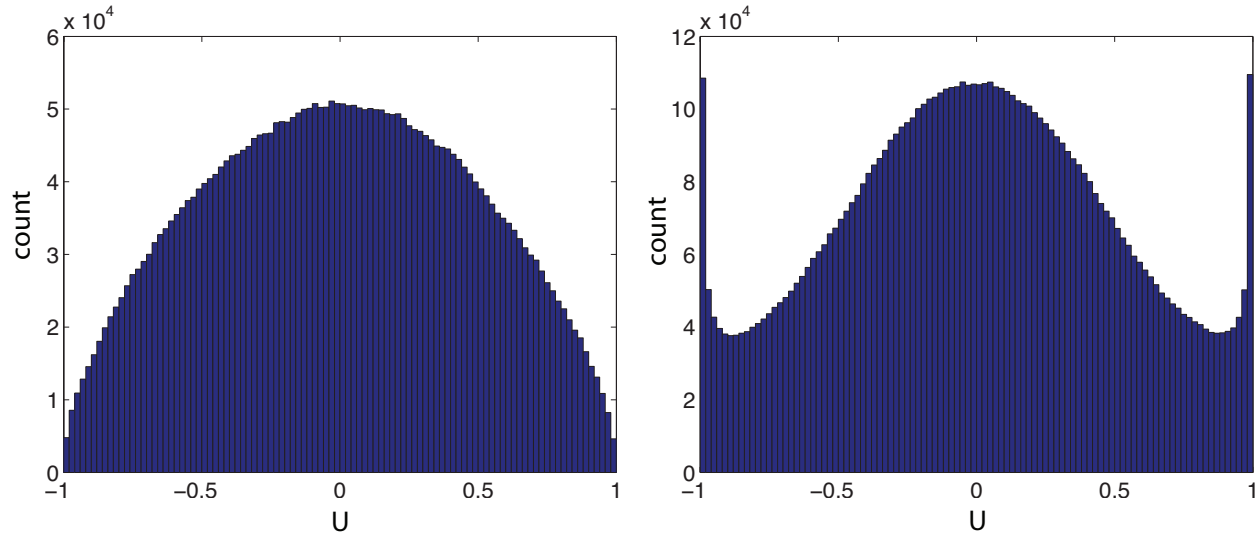

Figure 3.   Typical distribution histograms of the dispersion functions within an uncertainty interval of ± 1 when using the redraw method (left) and the scaling method (right).

Figure 3 illustrates the difference in the distribution of the dispersed functions within the uncertainty bounds when using the redraw method versus the scaling method. These histograms show how a large number of dispersions covers the uncertainty band (normalized here between ± 1). In the case of the traditional dispersion method with a random factor picked using a uniform distribution, the histogram would be flat with equal probability at every value within the uncertainty interval. For a measure of how these models stress the limits of the uncertainty interval, one can compute the probability of a dispersed function to reach 90% of the positive uncertainty. For a symmetric uniformly distributed uncertainty, this probability is trivially 1/20. When using the new method, one can generate a large number of dispersion functions (on the order of 10^5 dispersions) and then calculate what this probability is. When using the redraw method, this probability was calculated to be approximately 1/65 and, when using the scaling method, it was estimated to be 1/25. For added conservatism, one can use the scaling method to stress the model more at its uncertainty bounds. However, even though the exact distribution of the dispersed functions can be more easily controlled when using the traditional dispersion method, it can be argued that the effect of the distribution has less of an impact on the flight simulations than the modeling of the dispersions itself (i.e., bias vs. random). In cases where conservatism is preferred, the scaling method will provide a similar probability of stressing the model at the bounds of the uncertainty interval as that of the traditional method.

One of the most beneficial aspects of the new method is the inclusion of physics within the model. The incorporation of a series with a finite order and a bias limit, both determined non-arbitrarily, enables the data itself to guide how the dispersion model is built, rather than prescribing a rigid and often non-realistic model to all vehicles and all aerodynamic quantities. Each vehicle or quantity, therefore, has a tailored model that enables a more faithful representation of what could happen during flight. In the following section, a practical example of the new dispersion method applied to a NASA launch vehicle development is shown,

American Institute of Aeronautics and Astronautics

and the impact of the different modeling on the flight simulations reported.

II.   Practical Application

A.   Introduction

This section describes how the new dispersion method was developed and implemented for dispersing the aerodynamic rolling moment on the Ares I Crew Launch Vehicle, as part of the Constellation Program. Rolling moment is the aerodynamic moment that is exerted along the longitudinal axis of the launch vehicle, making the vehicle roll around that axis if it is not actively countered using roll control thrusters. On the Ares I Launch Vehicle, since the main engine is approximately in-line with the center of gravity of the vehicle, the gimbaling motion of the motor does not provide roll control. The vehicle, therefore, needs to be controlled using auxiliary roll control systems (RoCS), which are mounted on the side of the vehicle. More accurately predicting the magnitude of the rolling moment incurred by the vehicle and avoiding hyper-conservatism when designing the roll control systems could allow for smaller units, i.e., less extra weight thus more payload.
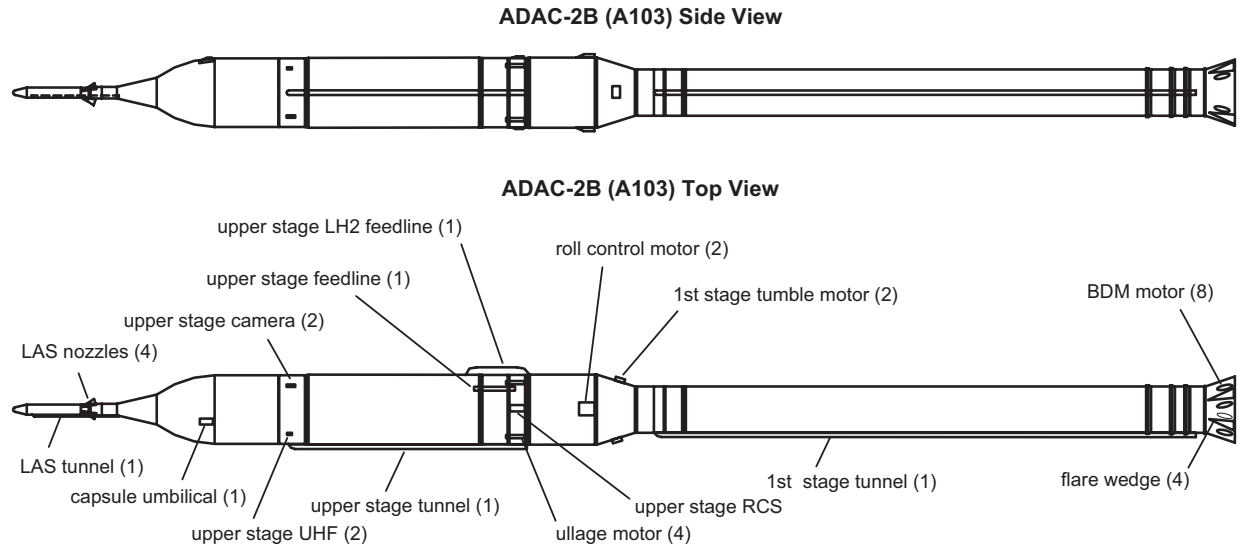
ADAC-2B (A103) Side View

ADAC-2B (A103) Top View

Figure 4. Side and top views of the Ares I crew launch vehicle with the description of the main protuberances present on the A103 configuration.

For a simplified axisymmetric launch vehicle at a given attitude and free-stream flow condition, with one longitudinally symmetric protuberance (non-cambered), the rolling moment coefficient integrated over all aerodynamic roll angles, $0 < \phi_a < 2\pi$, should be equal to zero, as derived here:

$$\int_0^{2\pi} C_l(\phi_a)d\phi_a = \int_0^{\pi} C_l(\phi_a)d\phi_a + \int_{\pi}^{2\pi} C_l(\phi_a)d\phi_a = \int_0^{\pi} C_l(\phi_a)d\phi_a + \int_{\pi}^{0} -C_l(\phi_a)d\phi_a = 0 \qquad (4)$$

In a more general case where the launch vehicle exhibits multiple longitudinally symmetric protuberances, as seen in Fig. 4, the aerodynamic interactions between them could, in effect, induce a small non-zero net rolling moment when integrated over all roll angles. In the case of a vehicle like the Ares I Crew Launch Vehicle, that non-zero value is very small, as measured during multiple wind tunnel tests and CFD simulations.[3,4,5] This means that the aerodynamic effect of the interactions between the various protuberances is of second order effect. Additionally, rolling moment uncertainty limits were calculated to be symmetric about the nominal rolling moment data. Even though the nature and magnitude of the aerodynamic uncertainties has no impact on the applicability of the proposed method and is not discussed in this paper, the reader is referred to Hemsch et al.[6] for more details on the uncertainty analysis process used to result in these uncertainty bounds. Figure 5 shows a nominal rolling moment trend as a function of aerodynamic roll angle

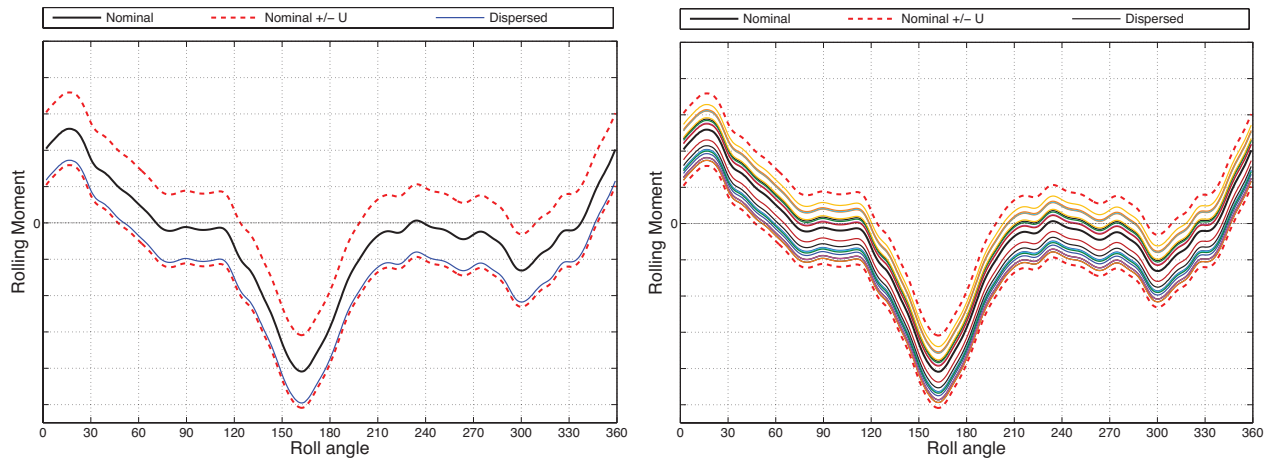American Institute of Aeronautics and Astronautics

Figure 5. Nominal Ares I rolling moment data (black) with symmetric uncertainty bounds (red dashed), with one (left) and twenty (right) traditional Monte-Carlo dispersed functions.

at a fixed Mach number and total angle of attack. The computed uncertainty in the data is also shown in red dashed lines. The integral of the rolling moment over all roll angles is small. It is, therefore, not physically realistic to disperse the data within the uncertainty bounds by imposing a bias up or down of the rolling moment coefficient as shown in Fig. 5. These biases can lead to significant non-zero values of rolling moment integrated over all aerodynamic roll angles in each dispersed function. The traditional model thus assumes that 100% of the computed uncertainty is attributed to a bias-type uncertainty, despite the fact that there is physical evidence, on this particular launch vehicle, that shows that only a small percentage of the uncertainty should, in fact, be attributed to bias error. The traditional dispersion model therefore lacks the physical modeling that would make all dispersions more realistic and constrain the dispersions to follow this physical reasoning. In addition, the traditional model imposes slopes and peak locations to be identical in every dispersion, as seen in Fig. 5. The aerodynamic dispersions do not stress the derivative quantities nor the phase-space within the model. This is one of the inherent limitations of the traditional dispersion method. The new method, presented in the previous section and demonstrated on actual data in the following section, allows for both nominal and derivative data dispersions, as well as phase shifts within the uncertainty bounds.

B.   Implementation

As previously argued, the bias limit L_b for aerodynamic rolling moment in the case of the Ares I launch vehicle was chosen to be *zero* so that all dispersed functions would integrate to the same value as the nominal function. Analysis of experimental and computational data from Ares I testing and simulations led to the selection of a third-order Fourier series model, as shown in Eq. 5. Indeed, Fig. 5 shows that the nominal function exhibits approximately six local extrema, and the order N of the Fourier series should, therefore, be 3, as described in Section I.B.:

$$
\begin{aligned}
g(\bar{\phi}_a) = &\, a_1 \, sin \left(2\pi \, (\bar{\phi}_a + h_1)\right) + b_1 \, cos \left(2\pi \, (\bar{\phi}_a + h_1)\right) \\
&+ a_2 \, sin \left(2\pi \, (2\bar{\phi}_a + h_2)\right) + b_2 \, cos \left(2\pi \, (2\bar{\phi}_a + h_2)\right) \\
&+ a_3 \, sin \left(2\pi \, (3\bar{\phi}_a + h_2)\right) + b_3 \, cos \left(2\pi \, (3\bar{\phi}_a + h_2)\right)
\end{aligned}
\tag{5}
$$

where $\bar{\phi}_a$ is the normalized aerodynamic roll angle defined as $\bar{\phi}_a = \phi_a/360$ with ϕ_a in degrees varying between 0 and 360°. Figure 6 shows a comparison of a randomly generated dispersion function for the traditional and new dispersion models. As expected, the traditional model shows a constant bias dispersion function, with a non-zero integrated value. The new dispersion shows more randomness, a periodicity of 360° with the values at 0 and 360° coinciding by construction, as well as an integrated value identically equal to zero. Figure 7 shows two sets (one of 5 and the other of 20) randomly generated dispersion functions. All of them

American Institute of Aeronautics and Astronautics

are periodic and integrate to zero by construction.

From Eq. 2, with $L_b = 0$, the dispersed rolling moment coefficient is equal to:

$$\widetilde{C_l}(x) = C_l(x) + g_i(x)\ U \tag{6}$$

where $C_l(x)$ is the rolling moment coefficient, and U is the uncertainty in rolling moment coefficient (constant in this case).
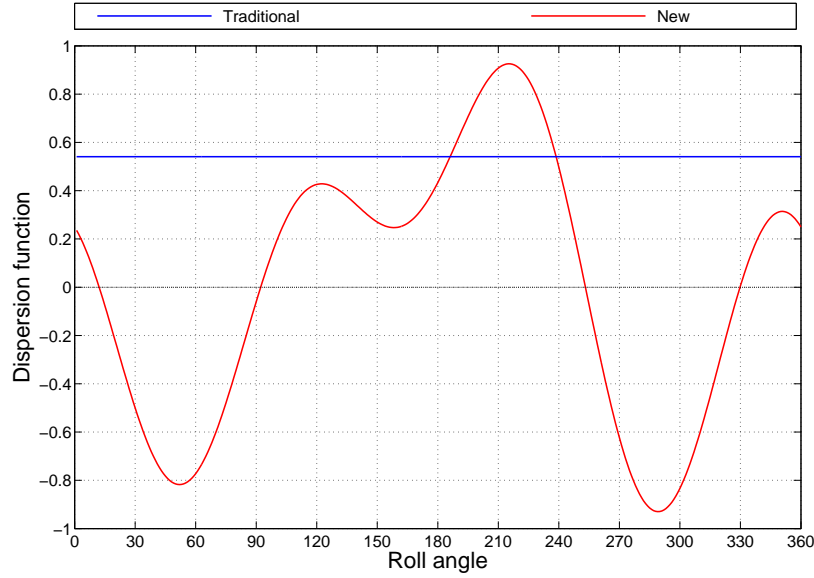

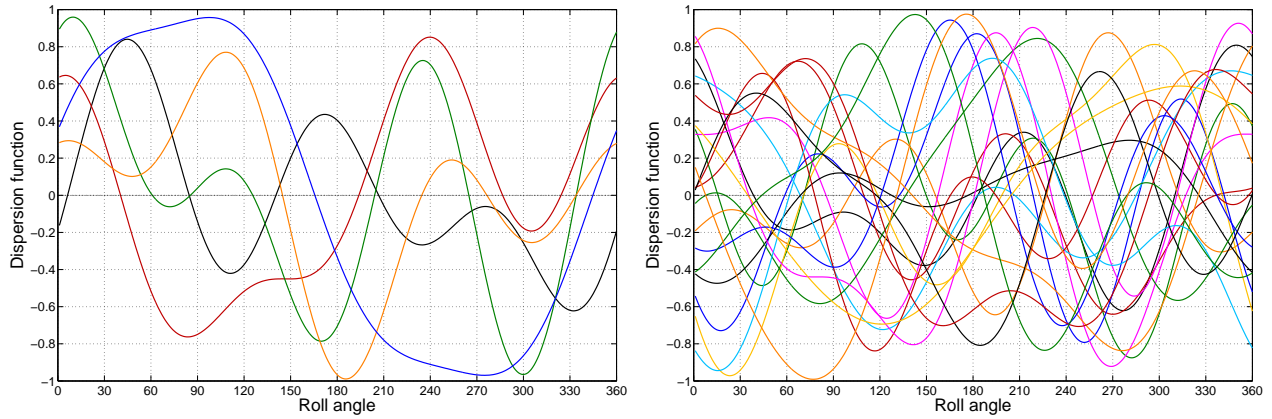**Figure 6. Comparison of traditional (blue) and new (red) dispersion model.**

Figure 7. Five (left) and twenty (right) randomly generated dispersion functions.

When applied to the nominal function, as described in Eq. 5 and displayed in Fig. 8, the dispersed data now shows *variations* around the nominal function rather than only positive and negative *offsets* about the nominal function. The new dispersed functions exhibit gradient variations at any given roll angle, as well as phase shifts of local extrema. By construction, each one of the dispersed functions also integrates to the same value as the nominal function, which does not allow for roll rates to build up during flight simulations because of the artificial constant biases in the dispersed aerodynamic rolling moment.
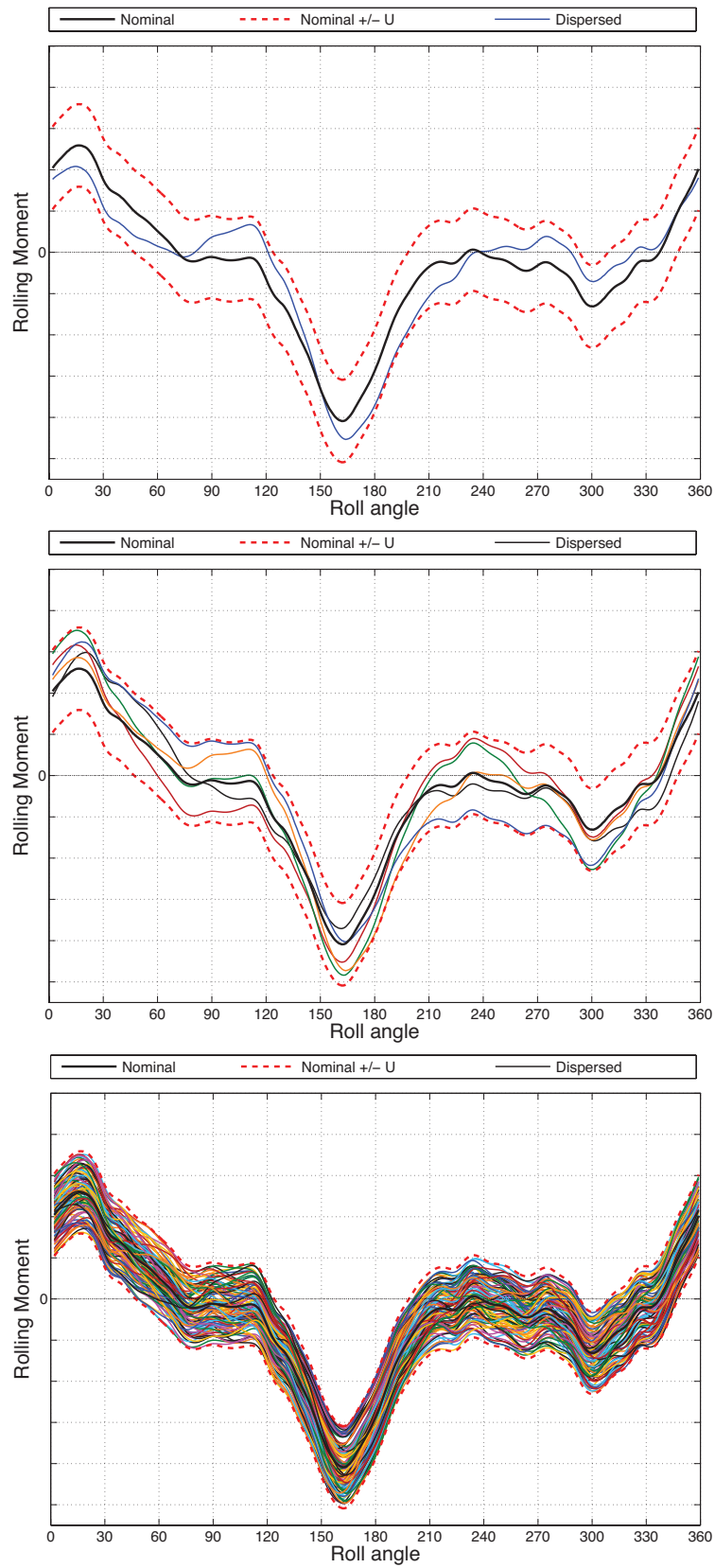
American Institute of Aeronautics and Astronautics

Figure 8. One (top), five (middle), and one hundred (bottom) dispersed rolling moment functions using the new dispersion method.

C. Simulation Results

Many parameters are randomly dispersed to complete a single Monte Carlo flight simulation. Indeed, aerodynamics is only one of many inputs to the simulated flight of a launch vehicle. Other inputs include mass properties of the vehicle, propulsion variabilities due to ambient temperature and burn-out dispersions, winds aloft, etc. On the order of a hundred random parameters are typically generated and kept constant for each Ares I flight simulation. Following the traditional dispersion method, once a dispersion factor is generated for rolling moment, as shown in Fig. 6, the entire flight simulation will be run using this value for rolling moment. Since the dispersion factor is modeled as being constant as a function of roll angle, and since rolling moment uncertainty magnitude is constant as a function of roll angle (it only depends on Mach number), the error introduced by the Monte Carlo simulation is an offset that only varies slowly as Mach number increases during ascent, as shown in Fig. 9.
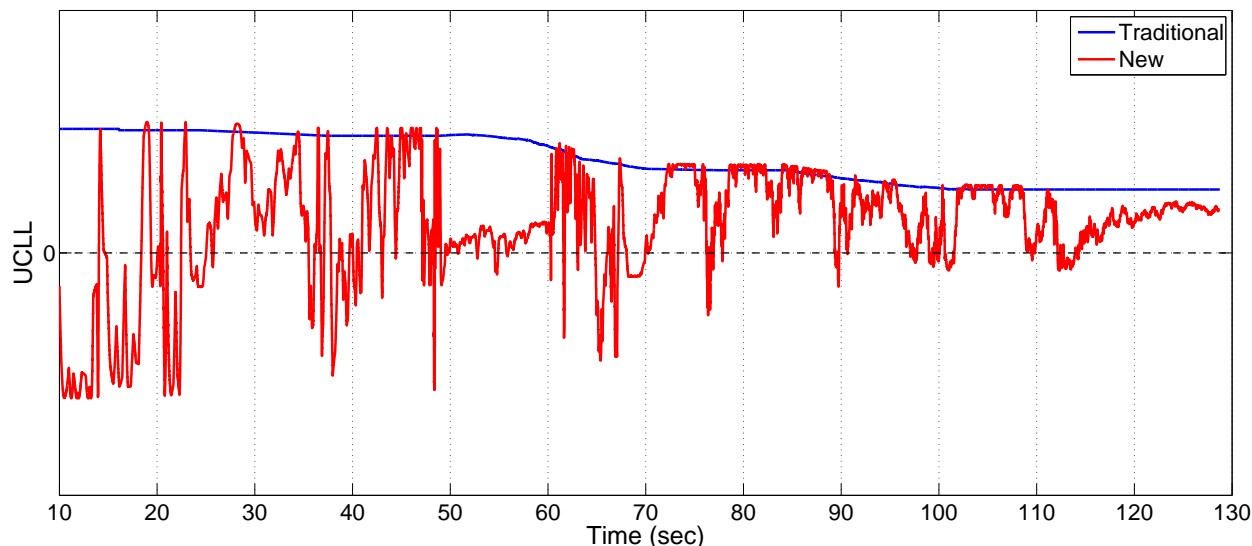

Figure 9. Comparison of Ares I rolling moment coefficient error UCLL (off nominal value) during one Monte Carlo flight simulation (from launch to stage separation), using the traditional method (blue) and the new method (red). Simulations provided by Steven Hough and Chong Lee from the NASA Marshall Space Flight Center.

It should not be expected that, during an entire flight, rolling moment error would be an offset, but rather a quantity that oscillates between positive and negative values within the uncertainty band because of a combination of many inputs of unknown magnitudes (winds, gusts, aeroelastic effects, jet interactions, turbulence, etc). By implementing the new method that makes the dispersion factor a function of roll angle, as shown in Eq. 5, the rolling moment error now varies in a much more random fashion and oscillates between positive and negative values as the aerodynamic roll angle of the vehicle varies between 0 and 360°. Indeed, since the vehicle flies at an angle of attack very close to zero, the resulting aerodynamic roll angle is likely to vary within the entire 0 to 360 degree range. Figure 9 shows in blue the error in rolling moment introduced in a Monte Carlo simulation, as implemented with the new method. This type of random behavior for input error in rolling moment seems to be more realistic and is closer to an engineer's expectations from a typical flight with many random inputs. To investigate the impact of using the new rolling moment dispersion method as compared to the traditional bias method from a potential gain perspective, 2000 flight simulations were run on the Ares I-X Flight Test Vehicle with the roll control motors turned off, using, on the one hand, the traditional dispersion method and, on the other hand, the scaling version of the new method, as described in Section I.B. The vehicle roll rate at stage separation was computed for each Monte Carlo dispersion to investigate how the difference in rolling moment dispersion modeling affected the vehicle when integrated over the entire flight. Figure 10 shows the normalized vehicle roll rates (i.e., roll rate divided by the maximum roll rate from the traditional method) for all 2000 individual dispersions using the traditional method (in blue) and the new method (in red). It is observed that the maximum predicted roll rates at stage separation were reduced by as much as 60% with the implementation of the new approach, indicating
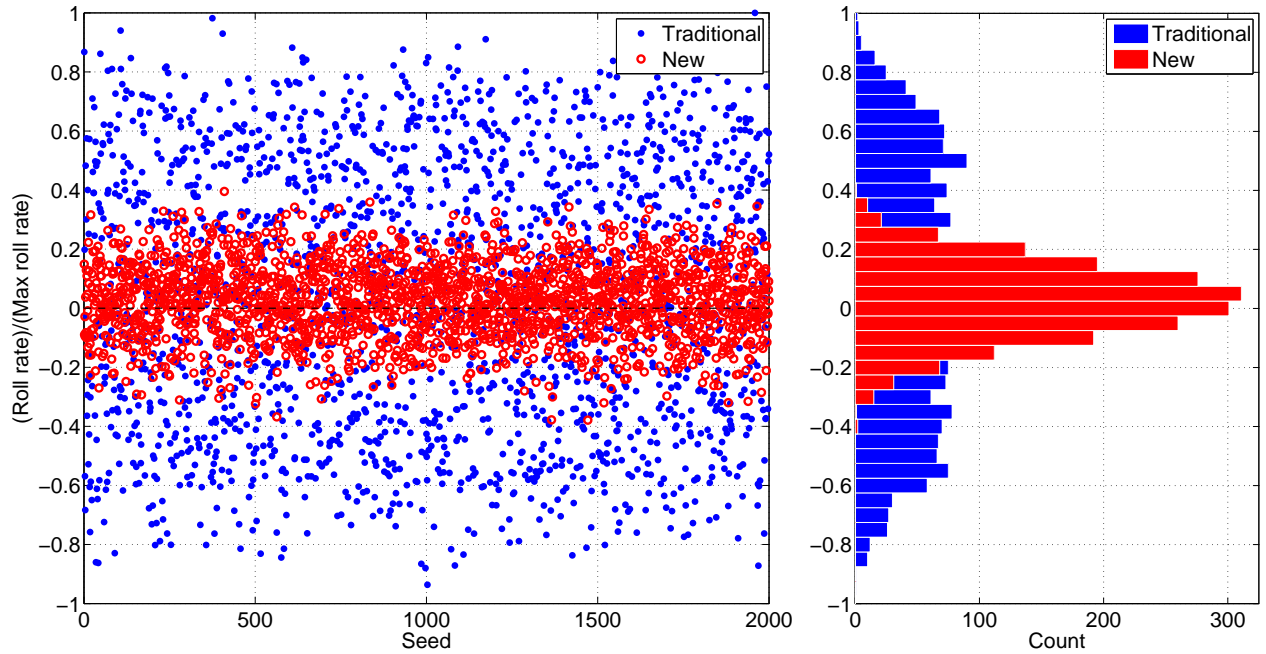
American Institute of Aeronautics and Astronautics

Figure 10. (left) Comparison of Ares I-X normalized roll rates at stage separation with no roll control from Monte Carlo simulations, using the traditional method (blue) and the new method (red); and (right) distribution histograms of the roll rates at stage separation. Simulations provided by Steven Hough and Chong Lee from the NASA Marshall Space Flight Center.

that the previous dispersion model was indeed hyper-conservative. By making the rolling moment error a positive or negative offset during the whole flight (as shown in Fig. 9), the traditional approach can, in many cases, force the vehicle to artificially build-up a roll rate during the entire ascent.

This method was proposed to the Ares I Aero Panel and Ares I GNC team as a possible alternative to the traditional dispersion method. After being approved by the panel as the new default dispersion method for aerodynamic rolling moment, it was implemented by the GNC team, and the results presented here were delivered within two weeks of its presentation. Its implementation does not require significant changes in the way Monte Carlo simulations are run in most projects at NASA. These results have had a significant impact on the NASA Ares I Project as far as roll control requirements are concerned. It is now recognized that the effective aerodynamic rolling moment dispersions experienced during atmospheric flight will not make this particular launch vehicle spin around its longitudinal axis, as previously shown by some of the traditional Monte Carlo dispersions. Smaller roll control motors can therefore be used and, in turn, payload mass can be increased. Additionally, the risk to the mission introduced by flying the flight test vehicle with no roll control motors (for cost-saving purposes) has been, consequently, lowered.

III.   Other Applications

Efforts to generalize the use of this method to all aerodynamic quantities is underway. It is foreseen that such a method could be beneficial in cases where the simulations are more sensitive to slope changes than magnitudes of a given quantity. For launch abort type vehicles and crew modules, aerodynamic pitching moment is a crucial quantity for controlling the flight vehicle around small angles of attack and during reorientation phases, especially since static stability margins are typically small on such vehicle configurations. Several programs throughout the agency have shown interest in applying the technique for these purposes. The Max Launch Abort System (MLAS) Project led by the NASA Engineering and Safety Center has accepted this method as the new default for aerodynamic rolling moment and is in the process of implemented the technique for dispersing all aerodynamic forces and moments. The Orion Launch Abort System and

American Institute of Aeronautics and Astronautics

Crew Module projects have also expressed strong interest in applying such a technique to improve the fidelity of the flight simulations and remove any over-conservatism caused by large biases in the dispersions.

This type of method could furthermore be beneficial in any area that has data combined with uncertainty about this data as an input to a model and when some type of randomization is required like in a Monte Carlo type of analysis, or when the generation of multiple instances of the data within the uncertainty band can provide additional information about the system, like in the study of oscillatory systems and dynamic stability analysis.

IV.   Concluding Remarks

A new physics-based model for dispersing aerodynamic data within a given uncertainty band in Monte Carlo type flight simulations has been developed. It's implementation on aerodynamic rolling moment data in the context of the Ares I Crew Launch Vehicle and the Ares I-X Flight Test Vehicle Projects has provided significant results and has shown that the traditional methods being used have the tendency to result in unrealistic and, in the present case, hyper-conservative predictions. For other aerodynamic quantities like pitching moment, the traditional dispersion method could also lead to non-conservative results because the derivatives are not stressed, by nature of this method. The modeling of physics within the dispersed aerodynamic quantities brings an additional amount of realism to the dispersion methods traditionally employed within NASA projects and results in a significant positive impact on our ability to meet requirements tied to roll rate limits, while saving resources that would have otherwise been spent on larger roll control systems because of hyper-conservatism in the flight simulations. Direct effects of incorporating physics within Monte Carlo simulation models of aerodynamic data can, therefore, range from reducing risk to reducing flight control system size and, in turn, increasing payloads.

The new method proposed in this paper is a general mathematical approach that presents the potential of being applied to many problems, where data and uncertainties are used together to make predictions of the behavior of systems within uncertain environments. Several efforts are underway to explore the application of such a method to aerodynamic quantities other than rolling moment, to simulating noise in computational fluid dynamics calculations, and to structural dynamics problems, among others.

Acknowledgments

References

[1]Hanson, J. M. and Beard, B. B., "Applying Monte Carlo Simulation to Launch Vehicle Design and Requirements Verification," *AIAA Guidance, Navigation, and Control Conference*, AIAA 2010-8433, 2010.

[2]Walker, E. L., Hemsch, M. J., Pinier, J. T., Bibb, K. L., Chan, D. T., and Hanke, J. L., "Constellation Program Lessons Learned in the Quantification and Use of Aerodynamic Uncertainty," *29th AIAA Applied Aerodynamics Conference*, 2011.

[3]Pinier, J. T., Niskey, C. J., Hanke, J. L., and Tomek, W. G., "Ares I Aerodynamic Testing at the Boeing Polysonic Wind Tunnel," *49th AIAA Aerospace Sciences Meeting Including the New Horizons Forum and Aerospace Exposition*, AIAA 2011-0998, 2011.

[4]Erickson, G. E. and Wilcox, F. J., "Ares I Aerodynamic Testing at the NASA Langley Unitary Plan Wind Tunnel," *49th AIAA Aerospace Sciences Meeting Including the New Horizons Forum and Aerospace Exposition*, AIAA 2011-0999, 2011.

[5]Abdol-Hamid, K. S. and Ghaffari, F., "Overview of Ares-I CFD Ascent Aerodynamic Database Development and Analysis Based on USM3D," *49th AIAA Aerospace Sciences Meeting Including the New Horizons Forum and Aerospace Exposition*, AIAA 2011-0015, 2011.

[6]Hemsch, M. J., Hanke, J. L., Walker, E. L., and Houlden, H. P., "Detailed Uncertainty Analysis for Ares I Ascent Aerodynamics Wind Tunnel Database," *26th AIAA Aerodynamic Measurement Technology and Ground Testing Conference*, AIAA 2008-4259, 2008.